Plasma structure in a pulsed discharge environment

Jérôme Remy[1], Ludovic Biennier and Farid Salama

NASA Ames Research Center, Space Science Division, MS 245-6, Moffett Field,
CA 94035-1000, USA

E-mail: fsalama@mail.arc.nasa.gov

Abstract
A pulsed slit discharge nozzle (PDN) has been developed in our laboratory
to generate molecular ions in an astrophysically relevant environment. The
free cold molecular ions are formed through soft (Penning) ionization of the
neutral precursor molecules seeded in a supersonic free jet and are probed
with cavity ringdown spectroscopy. An attempt is made to characterize the
nature and the structure of the plasma that is generated in these experiments
to optimize the yield of formation of ions in the jet. The experimental
conditions are characterized by a strong pressure gradient in a short
discharge zone. We find that the plasma generated in the PDN source is best
characterized as an intense abnormal glow discharge and that its structure is
reduced to a negative glow and to dark zones near the electrodes. We have
calculated the parameters (length, thickness and cathode voltage fall) that
are associated with the Crookes dark space and the negative glow in the
plasma. We have also estimated the electron temperature (T_e) and density
(n_e) in the plasma. All these parameters are required to optimize the yield of
formation of ions and radicals in the jet expansions, a key requirement in our
experiments.

1. Introduction

A supersonic expansion coupled to an electronic discharge
represents an extremely valuable tool for the production and the
study of translationally and rovibrationally cold radicals and
ions [1, 2]. This type of molecular source is also particularly
adapted to the study of laboratory analogues of interstellar
molecules and ions. Long-slit discharge jet expansions provide
the proper environment to study the molecular species found
in diffuse interstellar clouds where densities range between
25 and 100 particles per cubic centimetre, temperatures are of
the order of 100 K and the particles are submitted to intense
stellar radiation and cosmic ray bombardment [3]. Polycyclic
aromatic hydrocarbons (PAHs) play an important role among
interstellar species and have been the target of extensive
laboratory studies [3]. PAHs are found in meteorites and
interplanetary dust particles. PAHs are also thought to carry the
ubiquitous unidentified infrared bands (UIBs) seen in emission
in a wide variety of interstellar and extragalactic environments

as well as some of the 300 diffuse interstellar bands (DIBs)
seen in absorption in the spectra of diffuse interstellar clouds.
We have recently measured the electronic absorption spectra of
PAHs ions in a free jet discharge [4]. These experiments have
led us to study the nature of the plasma environment in which
the molecular ions are generated in the hope of optimizing the
ionization yield. A quantitative and qualitative description
of the properties of the plasma is also a key requisite to
correctly assess the relevance of the ion formation mechanisms
to the astrophysical application. A plasma environment is
typically characterized by the density of charged particles (ions
and free electrons) in the gas and the electronic temperature.
While detailed information is available for plasmas used in
industrial applications (e.g. lighting, gas discharge lasers,
pollution control and reduction, material processing, [5]),
little seems to be known—as far as we can say—on plasmas
that are generated in free jet expansions coupled to a
discharge (i.e. 'cold' plasmas) motivating the work described
here. In section 2, we describe the experimental set-up and
discuss the parameters that are associated with the plasma
generated in the experiments. In section 3, a step-by-step

---

[1] Permanent address: TU/e Eindhoven, Applied Physics Department,
Den Dolech 2, 5600 MB Eindhoven, The Netherlands.

modelling of the plasma is attempted and, finally, in section 4 we discuss the results of the model and the implications for the study and the optimization of the yield of cold molecular ions.

2. Experimental

The experimental set-up has been described in detail in [4] and only a brief description is provided here, focusing on the elements that are necessary for the discussion of the characteristics of the plasma.

The apparatus consists of a pulsed discharge slit nozzle (PDN) mounted on a vacuum chamber and coupled to a high-finesse optical cavity. The gas expansion is evacuated perpendicularly to the expansion plane by a mechanical booster pump that is backed by a dry pump (Edwards EH-1200/GV-250, 250 litre s^{-1} pumping capacity).

In typical running conditions (1 atm backing pressure of Ar—99.985% purity), the PDN source produces an intense gas pulse of 1.2 ms duration with a 10 Hz frequency, generating a residual pressure of 150 mTorr in the chamber.

The plasma expansion generated by the PDN is probed by a cavity ringdown spectrometer several millimetres downstream with a sub-ppm to ppm sensitivity. The spectrometer is based on a Nd : YAG pumped 0.2 cm^{-1} linewidth, tunable pulsed dye laser for the injection of visible photons into the high-finesse cavity. The ring-down cavity is made of two concave, high reflective mirrors (∼99.98% reflectivity coefficient, Los Gatos Research) with a 6 m curvature radius that are mounted 55 cm apart. A photodetector, connected to a high-speed scope or A/D board, is used for the detection of the visible photons leaking out of the rear mirror of the cavity.

The pulsed discharge nozzle (PDN) combines an intense slit jet configuration with two knife-edge electrodes that produce a discharge in the stream of the planar expansion. In this configuration, the plasma is generated after expansion of the Ar gas. The two negatively biased stainless steel jaws (cathode) are mounted on each side of the 200 μm wide by 10 cm long slit and are 400 μm apart. They are insulated from the PDN assembly (anode) by a 1.5 mm thick insulator (Macor plate). A negative bias (−400 to −600 V) is applied simultaneously to both electrodes through two 1 kΩ ballast resistors while the source body is independently grounded via a small 50 Ω resistor to provide a current return path and a way to measure it. This configuration ensures that the electrons flow towards the grounded PDN assembly (anode) against the supersonic stream and that the positive ions travel downstream. It also ensures that the discharge remains strictly confined within the 200 μm slit and that the glow is uniform along the entire length of the 10 cm slit. The geometry of the PDN leads to a residence time of a few microseconds for the molecules in the active region of the discharge. Also, the confinement of the discharge to a small upstream region of the expansion leads to efficient rotational cooling of the ions and radicals generated in the plasma [1, 2, 6]. At typical backing pressure of Ar (760 Torr), the steep pressure gradient within the expansion leads to a pressure of 2 Torr near the cathode, 1.5 mm from the nozzle.

3. Results and discussion

3.1. Approach

Plasmas are commonly classified according to the density of the charge carriers and the thermal energy (temperature) of electrons in particular. The measurement of the current density is an expression of these intrinsic properties. Table 1 lists the characteristics (gas pressure, applied voltage and discharge current) of two classes of plasma that are close to the characteristics of the plasma generated in the PDN experiments. According to this classification, the plasma generated in the PDN source is clearly a glow discharge.

Although the expanded gas is a mixture of gaseous PAHs highly diluted in Ar (typical ratio of PAH : Ar of the order of 0.3%), throughout this paper, we have assumed that the properties of the plasma are defined by the nature and the properties of the carrier gas (Ar).

The regime of glow discharge can be further characterized by measuring the breakdown voltage as a function of the current as shown in figure 1(*b*): $I = f(U)$. The breakdown voltage is defined as the voltage at which the gas becomes conductive. When a sufficient number of ion–electron pairs are formed through ionization, the secondary emission process is initiated, helping maintain the current. Typical working voltage and current values (−500 V and 30 mA, respectively) correspond to a glow discharge in the abnormal regime [7] where the current increases proportionally to the applied voltage (compare figures 1(*a*) and (*b*)).

The glow discharge breakdown pattern is generally described by Paschen's law $V_b = f(p, d)$ (equation (1)) where the breakdown voltage V_b is a function of the product of the gas pressure p and the interelectrode distance d [8]:

$$V_b = \frac{Bp \cdot d}{\ln(Ap \cdot d) - \ln[\ln(1 + 1/\gamma)]} \tag{1}$$

where A and B are phenomenological constants associated with argon-type discharges and are equal to 1360 m^{-1} Torr^{-1} and 23 500 V m^{-1} Torr^{-1}, respectively [9]. γ is the secondary emission yield of stainless steel with a value of 1.1 [10] and is associated with the ion bombardment of the cathode. It has been shown [11] that the electron emission due to the bombardment of the cathode by ground state and metastable neutrals is negligible in glow discharge processes.

We have measured the breakdown voltage V_b at various values of the gas backing pressure. In the current configuration, the interelectrode distance, d, is set at 1.5 mm (see section 2). The measured values are reported in figure 2. The curve

Table 1. Typical parameters of plasma.

Low pressure glow discharge[a]	PDN plasma[b]	High pressure arc discharge[a]
$P = 1$ mTorr–1 Torr	$P = 2$–760 Torr[c]	$P = 760$ Torr
$T_e = 1$–10 eV	$T_e = ?$	$T_e = 0.1$–2.0 eV
$n_e = 10^8$–10^{13} cm^{-3}	$n_e = ?$	$n_e = 10^{14}$–10^{19} cm^{-3}
$I = 10^{-4}$–1 A	$I < 10^{-1}$ A	$I > 1$ A
$V = -400$ to -800 V	$V = -500$ V	$V < -100$ V

[a] Adapted from [9].

[b] This work.

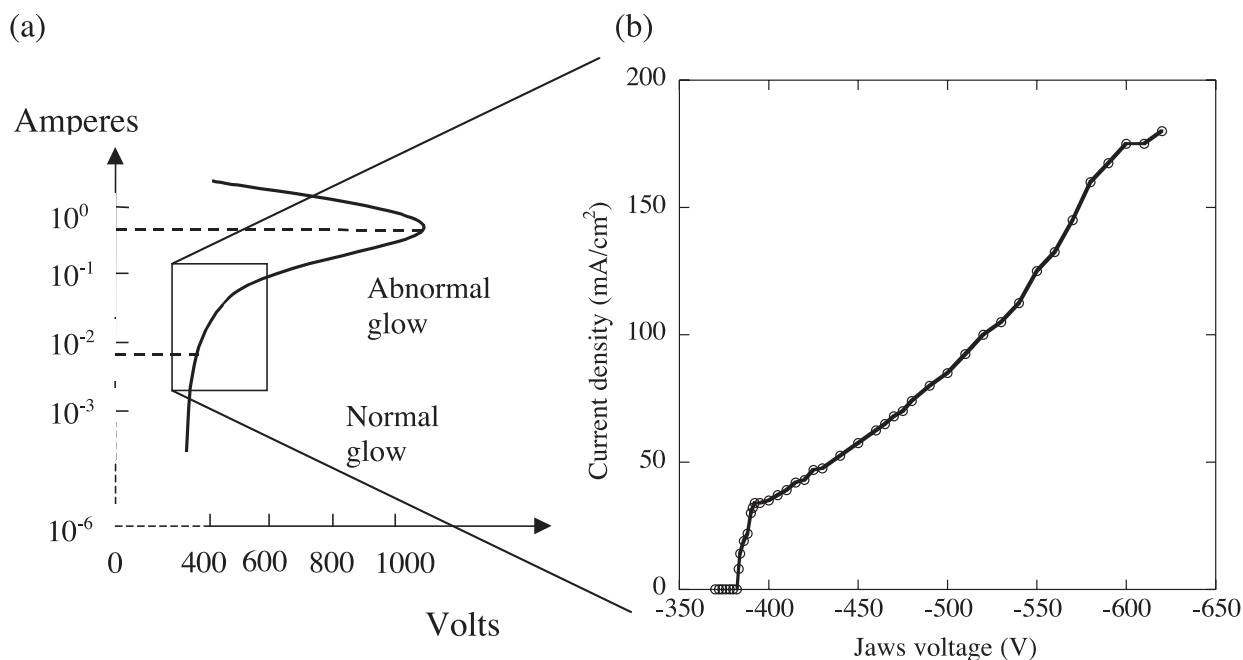[c] Pressure range within the 1.5 mm discharge region.

(a)

(b)

Figure 1. (*a*) Theoretical voltage–current characteristics of a DC discharge, (*b*) experimental measurements of the current density as a function of the discharge breakdown voltage.
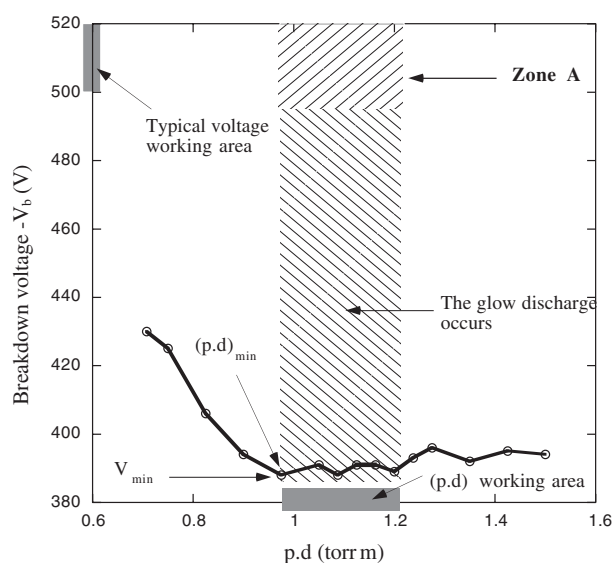

Figure 2. Breakdown voltage measured for the two stainless steel plane-parallel plates in the Ar jet expansion. Zone (A) indicates the zone where the density of Ar* becomes large enough to produce PAH ions at a detectable level (see text).

shows a single minimum breakdown potential $(V_b)_{min}$ and the corresponding minimum $(p \cdot d)_{min}$ product as expected for a glow discharge mode. It also leads (i) to an estimate of the minimum voltage required to generate a discharge in the jet at a given gas pressure and (ii) to information on the structure of the glow discharge (see discussion later). For example, the value of $(V_b)_{min}$ is -388 V and corresponds to the voltage threshold needed to generate a glow discharge within the argon gas at $(p \cdot d)_{min} = 650$ Torr $\times$ 1.5 mm $= 0.975$ Torr m. Since the typical backing pressure used in this paper ranges from about 650 to 800 Torr, $(p \cdot d)$ ranges between 0.9 and 1.2 Torr m

and (V_b) ranges from -388 to -391 V. Note that these are the conditions sufficient to generate a glow discharge in the PDN. They are not sufficient, however, to generate enough metastable Ar atoms to lead to the Penning ionization of the seeded PAH molecules [4] at detectable levels. Figure 2 also shows that under our working pressure conditions (p ranging from 650 to 800 Torr), $(p \cdot d)_{exp} \geqslant (p \cdot d)_{min}$. Under these conditions, the discharge zone is almost entirely occupied by the cathode region as discussed below (see figure 3(*a*)).

3.2. Structure of the glow discharge

Figure 3 contrasts the sequence of glowing and dark zones that commonly appear in normal glow discharges (figure 3(*a*), see, e.g. [12]) to the glow structure resulting from our experimental conditions (figures 3(*b*)–(*d*)). Here, two factors are primarily responsible for the formation of an abnormal glow discharge: the pressure regime and the short ($d = 1.5$ mm) interelectrode distance. There is a strong discharge pressure gradient in the free jet that ranges from 400–500 Torr at the anode to about 2–3 Torr at the cathode. Although the cathode dark space and negative glow seem to be unaffected by this environment, the positive column, the Faraday dark space, the Aston zone, the cathode layer and the anode glow all disappear. This only leaves the negative glow and dark spaces between the two electrodes [13]. We have observationally confirmed the absence of a positive column in the glow discharge. The glow is blue, red and green in the case of Ar, Ne and He, respectively, indicating the sole presence of a negative glow preceded by a Crookes (dark) zone where electrons are accelerated [14]. The steep pressure variation within the discharge zone makes it difficult to picture the glow discharge structure contrarily to the case of a typical DC discharge where the pressure remains constant over the entire interelectrode distance. We have chosen
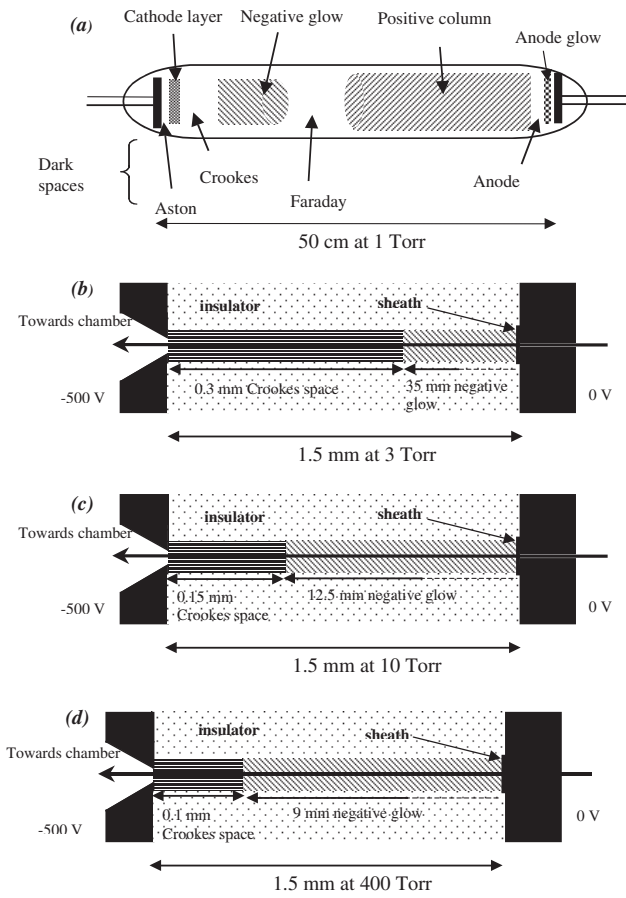
Figure 3. Glow discharge structure: (*a*) general case, (*b*)–(*d*) expected structures at constant pressures of 3 Torr, 10 Torr and 400 Torr, respectively.

to depict the glow structure at three representative pressure regimes: (i) at a high-pressure regime (400 Torr corresponds to the pressure 0.06 mm downstream), (ii) at an average pressure (10 Torr) that corresponds to the pressure at mid distance in between the electrodes (0.75 mm downstream) and (iii) at a low pressure regime (around 2–3 Torr) that corresponds to the pressure at the cathode (1.5 mm downstream). The characteristics of the discharge features that are associated with each of these pressure regimes are calculated in the diagram shown in figure 4 and are illustrated in figures 3(*b*)–(*d*).

3.2.1. Negative glow length (L). The length, L, of the negative glow was graphically determined from Brewer and Westhaver [15] who have measured L as a function of the cathode's dark zone potential drop (the abnormal cathode fall, V_{an}) for various gases. The cathode voltage fall V_{an} was calculated at each of the three pressure regimes defined above according to Aston's abnormal glow equation:

$$V_{an} = E + \frac{F\sqrt{j}}{p} \qquad (2)$$

where $E = 240$ and $F = 29\,400$ are dimensionless phenomenological constants associated with Ar, $j = 125$ mA cm^{-2} is the current density calculated for a current $i = 50$ mA and a plasma cross-section of 40 mm^2.
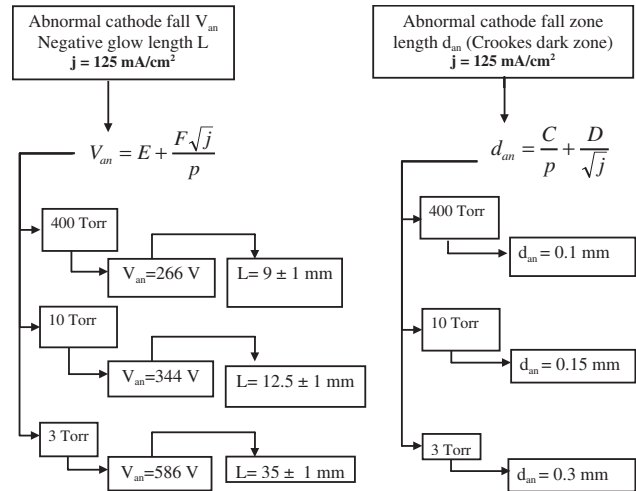

Figure 4. Structure of the plasma: Crookes dark space and negative glow calculations. Note that the abnormal cathode fall for the negative glow is higher than the voltage applied to the cathode. A common effect observed when there is a positive voltage across the negative glow (see, e.g. industrial lighting plasmas).

3.2.2. Crookes dark zone. The thickness of the Crookes dark zone is similarly calculated at the three pressure regimes following the equation:

$$d_{an} = \frac{C}{p} + \frac{D}{\sqrt{j}} \qquad (3)$$

where $C = 5.4$ and $D = 0.34$ are dimensionless phenomenological constants associated with Ar. The approach followed as well as the formulae used and the calculations performed are depicted in the diagram shown in figure 4.

In summary, an abnormal glow discharge is generated by the PDN source. The very short distance between the electrodes (1.5 mm) combined to the nature of the expanded carrier gas lead to a discharge where only two physical zones are expected to be present, namely, the Crookes dark zone and the negative glow.

The Crookes dark space is not completely dark, but it is much less luminous than the negative glow. In the abnormal glow regime, the glow extends over the entire surface of the cathode. Most of the potential difference between the two electrodes is concentrated in the Crookes dark zone, owing to the space charge of the positive ions. The negative glow is a plasma (i.e. virtually a field-free space) and electrons and positive ions are present in approximately the same number per cubic centimetre.

The potential difference across the dark space is large because the discharge itself has to extract electrons from the cathode. These primary electrons generate positive Ar ions along their path in the glow region. Argon ions will in turn strike the cathode and release secondary electrons. The strong electric field in the Crookes dark space region causes the major part of the electrons' path to be straight across the dark space along the field lines. The mean free path of the Ar atoms near the cathode (pressure close to a few Torr) is 5 mm whereas the mean free path of the electrons in the same region is 31 mm. Some of the electrons enter the negative glow with high velocities. There, they lose their energy in collisions
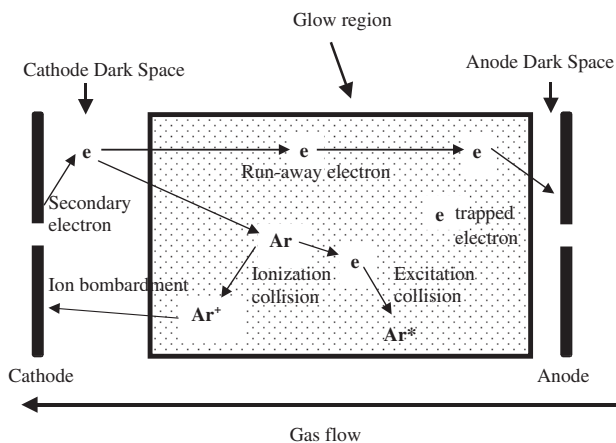
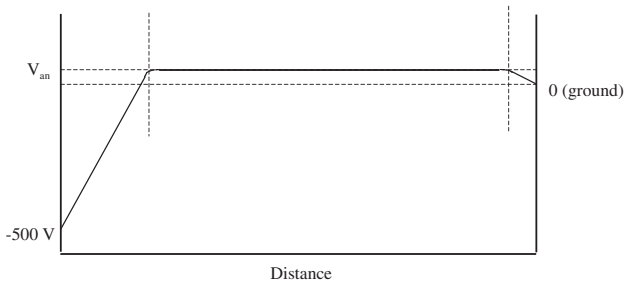**Figure 5.** Collision processes in a DC discharge.

Figure 6. Overview of the voltage distribution in the DC discharge (after Chapman [13]).

producing a mixture of ionized and metastable Ar atoms. This excitation is responsible for the negative glow. The electrons continue on their way towards the anode with lower velocities and make the anode side of the negative glow appear darker. The basic collision processes occurring in the discharge are depicted in figure 5.

The assumption that the negative glow is almost field-free requires the presence of a dark, negatively charged, sheath between the negative glow and the anode so that the anode remains grounded. This anode dark space is normally found to be thin, about one or two orders of magnitude less than the Crookes dark space [16]. Since the mean free path of the particles near the anode is in the micrometre range (21 μm for the Ar atoms and 123 μm for the electrons), the anode sheath is essentially collisionless and, in particular, not a source of ionization. The electric fields in the discharge are restricted to sheaths at each of the electrodes, as depicted in figure 6.

3.3. Plasma properties

3.3.1. Excitation temperature (T_{exc}). Spectroscopic diagnostics can be used to determine the electron temperature (T_e) in low temperature plasmas [16]. The absorption spectra of metastable Ar I lines provide information on the excitation temperature of the expanded Ar gas. We have measured the intensities of a series of metastable Ar I lines with cavity ring-down spectroscopy and applied the Boltzmann plot method to the resulting data (see [16] for a detailed discussion of the Boltzmann plot method). The laboratory spectra are shown in figure 7. The associated Boltzmann function,
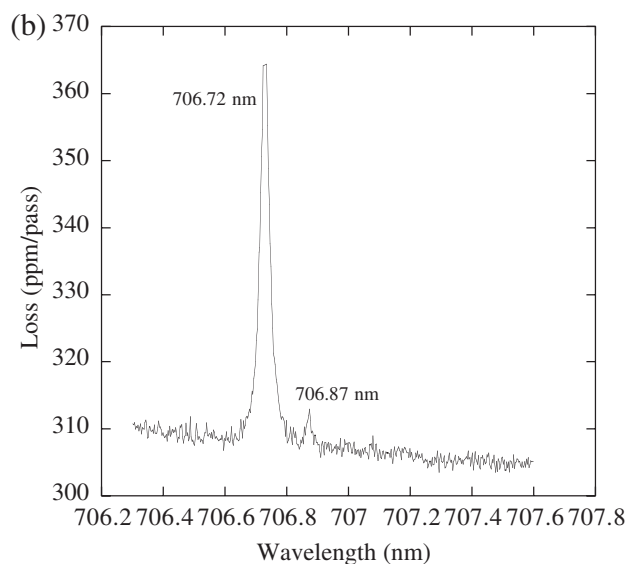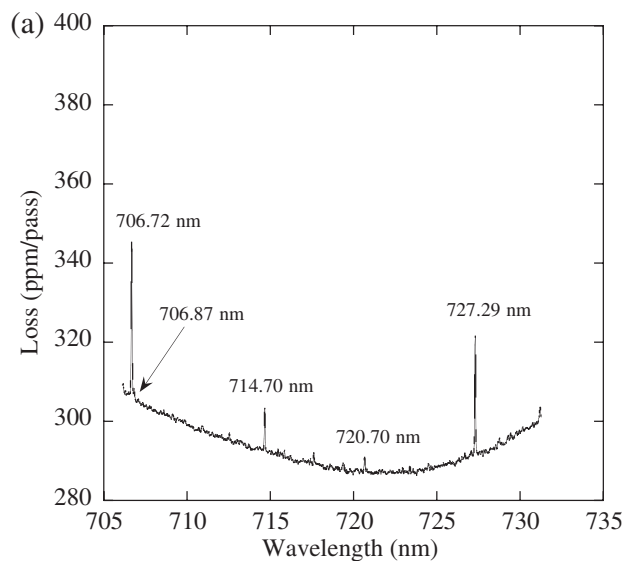

Figure 7. (*a*) PDN-CRDS absorption spectrum of pure Ar gas, (*b*) close-up on the 706.72 and 706.87 nm absorption lines of Ar I*. Note that the baseline of the spectrum has not been corrected for the response curve of the mirrors and for the additional losses due to scattering by the plasma.

$\ln[I_{12}\lambda_{12}/g_1 A_{12}] = f(E_1)$, is plotted in figure 8 where g_1 is the statistical weight of the lower level 1 of metastable Ar I, A_{12} is the transition probability from level 1 to level 2, λ_{12} is the wavelength for the transition 1–2, I_{12} is the corresponding intensity, and E_1 is the energy of the lower level (see table 2). The scattering seen in the plot is primarily due two factors: (i) the small energy gap between the atomic excited states that are involved in the transitions reported in figure 7 and in table 2 and, (ii) the low accuracy of the atomic transition value A_{12}. Ar II lines are not observed under the current experimental conditions. This is probably due to the weaker absorption cross-sections of Ar II lines in the wavelength range of observation and to a low population of Ar ions. This results in a smaller number of lines that are available for a Boltzmann plot diagnostic and, consecutively, to a decrease in the accuracy of the temperature that is derived from the measurements
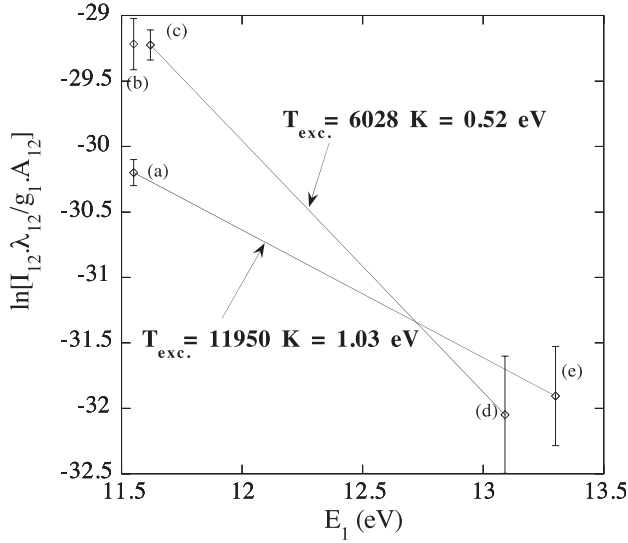
Figure 8. Boltzmann plot for Ar I* lines: (a) 706.72 nm, (b) 714.70 nm, (c) 727.29 nm, (d) 706.87 nm, (e) 720.70 nm. The transition lines are detailed in table 2.

Table 2. Ar I* transition lines (from NIST http://www.nist.gov).

Wavelength λ (nm)	Transition probability A_{lu} (s^{-1})	Statistical weight g_l	Lower energy E_l (cm^{-1})	Lower energy E_l (eV)
706.72	3.80×10^6	5	0.9314×10^5	11.55
706.87	1.20×10^6	5	1.0562×10^5	13.09
714.70	3.75×10^5	5	0.9314×10^5	11.55
720.70	1.49×10^6	5	1.0729×10^5	13.30
727.29	1.83×10^6	3	0.9375×10^5	11.62

[17]. The linear curve fit applied to the Boltzmann plot provides, nonetheless, an estimated excitation temperature T_{exc} that ranges between 6028 K (0.52 eV) and 11 950 K (1.03 eV). Assuming that the region of the jet that is probed by the laser is in a partial local thermal equilibrium (PLTE), one can derive $T_{\mathrm{e}} = T_{\mathrm{exc}}$.

3.3.2. Electronic density (n_{e}). The electronic density is derived from the current density measured for the discharge. Using the plasma resistivity, figure 1(*b*) provides an estimate of the electron density within the discharge region itself. Because of the isotropic nature of the discharge and the absence of magnetic field, the steady state Langevin equations for the electrons can be written as

$$-eE - m_{\mathrm{e}} \nu_{\mathrm{c}} u_{\mathrm{e}} = 0 \qquad (4)$$

where E is the constant and uniformly applied electric field ($E = V/d = 3333\,\mathrm{V\,cm^{-1}}$), e and m_{e} are the electron charge and mass, respectively, ν_{c} the collisionnal frequency and u_{e} the electron drift velocity.

We can solve equation (4) for u_{e}:

$$u_{\mathrm{e}} = \frac{-e}{m_{\mathrm{e}} \cdot \nu_{\mathrm{c}}} \cdot E = -\mu_{\mathrm{e}} \cdot E \qquad (5)$$

where $\mu_{\mathrm{e}} = e/m_{\mathrm{e}} \cdot \nu_{\mathrm{c}}$ is the electron mobility.

Assuming that all electrons move with the velocity u_e and that the neutrals involved in the collisions are at rest, electron–neutral collisions balance the applied electric field. The electron motion, neglecting the inertia of the relatively light electrons, is then:

$$J = -e \cdot n_{\mathrm{e}} \cdot u_{\mathrm{e}} \qquad (6)$$

where n_{e} is the electron density.

The gas is not fully ionized and most collisions occur between the electrons and the neutral Ar atoms. Therefore, combining equations (5) and (6) gives:

$$J = e \cdot n_{\mathrm{e}} \cdot \mu_{\mathrm{e}} \cdot E \qquad (7)$$

The electric field, E, and the current density, j, are experimental values derived from figure 1(*b*). The electron mobility μ_{e} depends on the density of neutrals (not electrons, see [13]) through the relation [18]:

$$\mu_{\mathrm{e}} = \mu_{\mathrm{e}_0} \cdot \frac{n_{\mathrm{L}}}{n_{\mathrm{Ar}}} \qquad (8)$$

where μ_{e_0} is the reduced electron mobility, which depends on the reduced electric field E/p and is equal to $410\,\mathrm{cm^2 V^{-1} s^{-1}}$ at a pressure of 400 Torr [18]. Loschmidt's number, n_{L}, is defined as the number of atoms in a gram-atom or the number of molecules in a gram-molecule and is equal to $2.69 \times 10^{19}\,\mathrm{cm^{-3}}$. The density, n_{Ar}, of Ar atoms calculated in the supersonic jet is equal to $9.8 \times 10^{17}\,\mathrm{cm^{-3}}$ at 3 Torr and to $1.8 \times 10^{19}\,\mathrm{cm^{-3}}$ at 400 Torr [19].

The electron density can now be derived from equation (7):

$$n_{\mathrm{e}} = \frac{j}{e \cdot \mu_{\mathrm{e}_0} \cdot (n_{\mathrm{L}}/n_{\mathrm{Ar}}) \cdot E} \qquad (9)$$

In the case of the low- and high-pressure regimes, electron density values range between $5.5 \times 10^9\,\mathrm{cm^{-3}}$ and $2.7 \times 10^{11}\,\mathrm{cm^{-3}}$, respectively. The upper limit of this value is consistent with the density of aromatic ions in the plasma region, $n_{\mathrm{PAH+}}$, that was derived from the measurement of the absorption spectra of selected PAH ions ($2 \times 10^{10}\,\mathrm{cm^{-3}} < n_{\mathrm{PAH+}} < 10^{12}\,\mathrm{cm^{-3}}$, [4]).

4. Conclusion

We have studied the nature and the structure of the plasma that is generated in our experiments where a pulsed discharge source is coupled to a pulsed free jet expansion. The experimental conditions are characterized by a strong pressure gradient in the discharge zone and a short interelectrode distance (the pressure varies from 500 to 2 Torr over the 1.5 mm interelectrode distance). The plasma generated in the PDN source is characterized as an intense glow discharge in the abnormal regime. The detailed structure of the glow discharge under such working conditions seems to be reduced to a negative glow and to dark zones near the electrodes. We have calculated the parameters (length, thickness and cathode voltage fall) that are associated with the two major zones (the Crookes dark space and the negative glow) in the plasma. We have also estimated the electron temperature (T_{e}) and density (n_{e}) in the plasma. All these parameters are required to quantitatively optimize the yield of formation of ions and radicals in the jet expansions, a key requirement in our astrophysically driven experiments.

Acknowledgments

References

[1] Anderson D T, Davis S, Zwier T S and Nesbitt D J 1996 *Chem. Phys. Lett.* **258** 207

[2] Davis S, Anderson D T, Duxbury G and Nesbitt D J 1997 *J. Chem. Phys.* **107** 5661

[3] Salama F 1999 *Solid Interstellar Matter: The ISO Revolution* (Les Houches, France: EDP Sciences) pp 65–87

[4] Biennier L, Salama F, Allamandola L J and Scherer J J 2003 *J. Chem. Phys.* **118** 7863

[5] 1995 *Plasma Science: From Fundamental Research to Technological Applications* (Washington, DC: National Academy Press) pp 33–46

[6] Liu K, Fellers R S, Viant M R, McLaughlin R P, Brown M and Saykally R 1996 *Rev. Sci. Instrum.* **67** 410

[7] Penning F M 1957 *Electrical Discharges in Gases* (New York: MacMillan) p 41

[8] Raizer Yu P 1997 *Gas Discharge Physics* 2nd edn (Berlin: Springer) pp 133–5

[9] Lieberman M A and Lichtenberg A J 1994 *Principles of Plasma Discharges and Material Processing* (New York: Wiley) pp 457–61

[10] Baglin V, Bojko1 J, Gröbner O, Henrist B, Hilleret N, Scheuerlein C and Taborelli M 2000 *Proc. EPAC (CERN, Vienna, Austria)*

[11] Medved D B and Strausser Y E 1965 *Adv. Electron. Electron Phys.* **21** 101

[12] Von Engel 1965 *Ionized Gases* (New York: Oxford University Press) p 218

[13] Chapman B 1980 *Glow Discharge Processes* (New York: Wiley) pp 78–81

[14] Brown S C 1966 *Introduction to Electrical Discharges in Gases* (New York: Wiley) p 214

[15] Brewer A K and Westhaver J W 1937 *J. Appl. Phys.* **8** 779

[16] Wiese W L 1991 *Spectrochim. Acta* B **46** 831

[17] Petzenhauser I, Ernst U, Hartmann W and Frank K 2001 *Arbeitsgemeinschaft Plasma Physik (Bad Honnef, Germany)*

[18] Delcroix J L 1966 *Physique des Plasmas 2* (Paris: Dunod) pp 113–17

[19] Miller D R 1988 *Atomic and Molecular Beam Methods* ed G Scoles (New York: Oxford University Press) pp 15–53